LU TP 00-34
Revised version
June 2, 2001

Hydrogen Bonds, Hydrophobicity Forces and the Character of the Collapse Transition

Anders Irbäck, Fredrik Sjunnesson and Stefan Wallin[1]

Complex Systems Division, Department of Theoretical Physics
Lund University, Sölvegatan 14A, S-223 62 Lund, Sweden
http://www.thep.lu.se/tf2/complex/

Contribution to *Proceedings of the ISI Workshop "Protein Folding: Simple Models and Experiments"*, Torino, April 27 - May 2, 2000.

Abstract:
We study the thermodynamic behavior of a model protein with 54 amino acids that is designed to form a three-helix bundle in its native state. The model contains three types of amino acids and five to six atoms per amino acid, and has the Ramachandran torsion angles as its only degrees of freedom. The force field is based on hydrogen bonds and effective hydrophobicity forces. We study how the character of the collapse transition depends on the strengths of these forces. For a suitable choice of these two parameters, it is found that the collapse transition is first-order-like and coincides with the folding transition. Also shown is that the corresponding one- and two-helix segments make less stable secondary structure than the three-helix sequence.

Keywords: protein folding, folding thermodynamics, hydrogen bonds, hydrophobicity

[1]E-mail: irback, fredriks, stefan@thep.lu.se

1 Introduction

The study of the formation of the native structures of proteins is hampered by computational limitations and uncertainties about the relevant forces, which makes model building a delicate and highly relevant task. Most current models use one or both of two quite drastic approximations, the lattice and Gō [1] approximations, where the latter amounts to ignoring interactions that do not favor the desired structure. Models of these types have provided valuable insights into the physical principles of protein folding [2–6], but have their obvious limitations.

Besides being computationally convenient, lattice models have the important advantage that it is known what is needed in order for stable and fast-folding chains to exist; it can be achieved by using a simple contact potential. For off-lattice models this is largely unknown, although one thing that seems clear is that it is not enough to simply use a potential analogous to the contact potential [7–9]. Because of this uncertainty, and because of evidence that the native structure in itself is a major determinant of folding kinetics [10], many off-lattice studies have been based on Gō-type potentials.

In this paper, we take a different approach, by discussing an off-lattice model, proposed in [11], that does not use the Gō approximation. In this model, the formation of a native structure is driven by hydrogen bonding and effective hydrophobicity forces. The model has three types of amino acids and the Ramachandran angles ϕ_i and ψ_i [12] as its degrees of freedom. Each amino acid is represented by five or six atoms.

Using this model, we study a three-helix-bundle protein with 54 amino acids, which represents a truncated and simplified version of the four-helix-bundle protein *de novo* designed by Regan and Degrado [13]. To study size dependence, we also look at the behavior of the corresponding one- and two-helix segments. The thermodynamic properties of these different chains are explored by using the method of simulated tempering [14–16].

Two key parameters of this model are the respective strengths $\epsilon_{\rm hb}$ and $\epsilon_{\rm AA}$ of the hydrogen bonds and hydrophobicity forces. For a suitable choice of these parameters, to be denoted by $(\tilde{\epsilon}_{\rm hb}, \tilde{\epsilon}_{\rm AA})$, the three-helix sequence is found to have the following properties [11]:

- It does form a stable three-helix bundle (except for a twofold topological de-

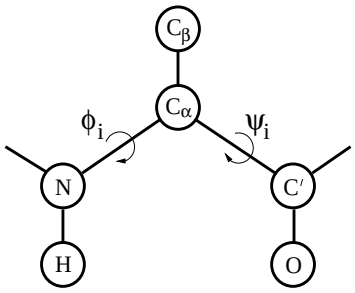

Figure 1: Schematic figure showing the representation of one amino acid.

generacy).

- It undergoes a first-order-like folding transition, from an expanded state to the native three-helix-bundle state.
- It forms more stable secondary structure than the one- and two-helix segments.

Qualitatively similar results have been obtained previously for C_α [6, 17–20] and all-atom [21] off-lattice chains, but, as far as we know, only with Gō-type potentials.

The paper is organized as follows. In Section 2, we give a brief description of the model. Our results are presented in Section 3. Here, we first summarize the results obtained in [11] for $(\epsilon_{\rm hb}, \epsilon_{\rm AA}) = (\tilde{\epsilon}_{\rm hb}, \tilde{\epsilon}_{\rm AA})$. We then discuss how the character of collapse transition depends on the relative strength of $\epsilon_{\rm hb}$ and $\epsilon_{\rm AA}$, by studying the behavior for $(\epsilon_{\rm hb}, \epsilon_{\rm AA}) = (\tilde{\epsilon}_{\rm hb} - \kappa, \tilde{\epsilon}_{\rm AA} + \kappa)$ for different κ. We end with a brief summary in Section 4.

2 The Model

The model we study is a reduced off-lattice model. Figure 1 illustrates the representation of one amino acid. The side chain is represented by a single atom, C_β, which can be either hydrophobic, polar or absent. This gives us three types of amino acids: A with hydrophobic C_β, B with polar C_β, and G (glycine) without C_β.

The H, O and C_β atoms are all attached to the backbone in a rigid way. Furthermore, in the backbone, all bond lengths, bond angles and peptide torsion angles (180°)

are held fixed. This leaves us with two degrees of freedom per amino acid, the Ramachandran torsion angles ϕ_i and ψ_i (see Figure 1).

Our energy function

$$E = E_{\rm loc} + E_{\rm sa} + E_{\rm hb} + E_{\rm AA} \tag{1}$$

is composed of four terms. The local potential $E_{\rm loc}$ has a standard form with threefold symmetry,

$$E_{\rm loc} = \frac{\epsilon_\phi}{2}\sum_i (1+\cos 3\phi_i) + \frac{\epsilon_\psi}{2}\sum_i (1+\cos 3\psi_i)\,. \tag{2}$$

The self-avoidance term $E_{\rm sa}$ is given by a hard-sphere potential of the form

$$E_{\rm sa} = \epsilon_{\rm sa}\sum_{i<j}{}' \left(\frac{\sigma_{ij}}{r_{ij}}\right)^{12}, \tag{3}$$

where the sum runs over all possible atom pairs except those consisting of two hydrophobic C_β. The hydrogen-bond term $E_{\rm hb}$ is given by

$$E_{\rm hb} = \epsilon_{\rm hb}\sum_{ij} u(r_{ij})v(\alpha_{ij},\beta_{ij})\,, \tag{4}$$

where

$$u(r_{ij}) = 5\left(\frac{\sigma_{\rm hb}}{r_{ij}}\right)^{12} - 6\left(\frac{\sigma_{\rm hb}}{r_{ij}}\right)^{10} \tag{5}$$

$$v(\alpha_{ij},\beta_{ij}) = \begin{cases} \cos^2\alpha_{ij}\cos^2\beta_{ij} & \alpha_{ij},\beta_{ij} > 90^\circ \\ 0 & \text{otherwise} \end{cases} \tag{6}$$

Here, i and j represent H and O atoms, respectively, and r_{ij} denotes the HO distance, α_{ij} the NHO angle, and β_{ij} the HOC$'$ angle. The last term in Equation 1 is the hydrophobicity energy $E_{\rm AA}$, which has the form

$$E_{\rm AA} = \epsilon_{\rm AA}\sum_{i<j}\left[\left(\frac{\sigma_{\rm AA}}{r_{ij}}\right)^{12} - 2\left(\frac{\sigma_{\rm AA}}{r_{ij}}\right)^{6}\right], \tag{7}$$

where both i and j represent hydrophobic C_β. To speed up the simulations, a cutoff radius r_c is used,[2] which is 4.5Å for $E_{\rm sa}$ and $E_{\rm hb}$, and 8Å for $E_{\rm AA}$.

The parameters of the energy function were determined empirically based on the shape of the Ramachandran ϕ_i, ψ_i distribution and on the overall thermodynamic behavior of the three-helix-bundle protein. A complete list of energy and geometry

[2]The cutoff procedure is $f(r) \mapsto \tilde{f}(r)$ where $\tilde{f}(r) = f(r) - f(r_c) - (r-r_c)f'(r_c)$ if $r < r_c$ and $\tilde{f}(r) = 0$ otherwise.

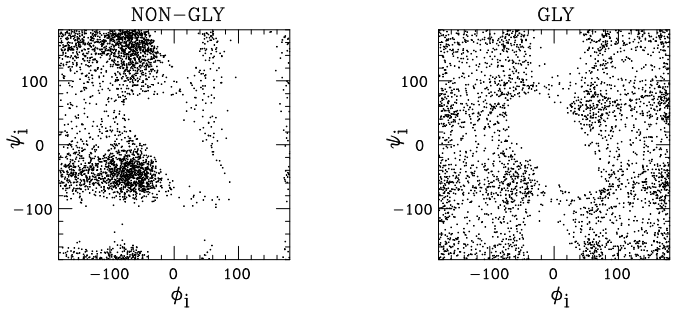

Figure 2: ϕ_i, ψ_i scatter plots for non-glycine and glycine, as obtained by simulations of the chains GXG for X=A/B and X=G, respectively, at $kT = 0.625$ (shown is ϕ_i, ψ_i for X).

1H:	BBABBAABBABBAABB
2H:	1H–GGG–1H
3H:	1H–GGG–1H–GGG–1H

Table 1: The sequences studied.

parameters can be found in [11]. In Figure 2, we show the final ϕ_i, ψ_i distributions for non-glycine (A and B) and glycine.

As mentioned in the introduction, we study the model for different $(\epsilon_{\rm hb}, \epsilon_{\rm AA})$. For $(\epsilon_{\rm hb}, \epsilon_{\rm AA}) = (\tilde{\epsilon}_{\rm hb}, \tilde{\epsilon}_{\rm AA}) = (2.8, 2.2)$ (dimensionless units), it turns out that

$$\tilde{\epsilon}_{\rm hb}/kT_{\rm f} \approx 4.3 \qquad \tilde{\epsilon}_{\rm AA}/kT_{\rm f} \approx 3.4\,, \tag{8}$$

where $T_{\rm f}$ denotes the folding temperature of the three-helix-bundle protein (see below).

The three sequences studied are listed in Table 1. They contain 16, 35 and 54 amino acids, respectively. The one-helix segment 1H consists of A and B amino acids that are distributed in such a way that this segment can form a helix with all hydrophobic amino acids on the same side. The three-helix sequence, 3H, consists of three such stretches of As and Bs plus two GGG segments.

There have been several earlier studies of similar-sized helical proteins using models at comparable levels of resolution [18, 22–27]. Among these studies, most similar to ours is that of Takada et al. [27]. These authors studied the same sequences, using a somewhat similar chain representation and a different, more elaborate force field.

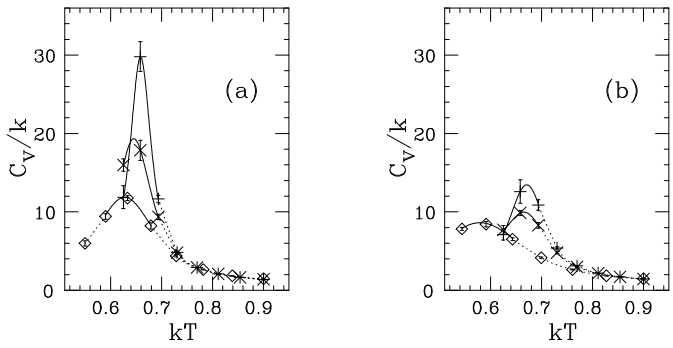

Figure 3: The specific heat $C_v = (\langle E^2\rangle - \langle E\rangle^2)/NkT^2$ against temperature for the sequences 1H ($\diamond$), 2H ($\times$) and 3H ($+$) (see Table 1), for (a) $\kappa = 0$ and (b) $\kappa = 0.3$ (N denotes the number of amino acids). The full lines represent single-histogram extrapolations [28]. Dotted lines are drawn to guide the eye.

3 Results

Using simulated tempering, we study the thermodynamic behavior of the chains defined above for

$$\epsilon_{\rm hb} = \tilde{\epsilon}_{\rm hb} - \kappa \qquad\qquad \epsilon_{\rm AA} = \tilde{\epsilon}_{\rm AA} + \kappa \tag{9}$$

for different κ.

3.1 Balance between Hydrogen Bonds and Hydrophobicity Forces

We begin with a summary of the results obtained in [11] for $\kappa = 0$.

For this choice of $(\epsilon_{\rm hb}, \epsilon_{\rm AA})$, it turns out that the three-helix sequence exhibits an abrupt collapse transition, signaled by a sharp peak in the specific heat. This can be seen from Figures 3a and 4, which show the specific heat and radius of gyration, respectively, against temperature.

It is instructive to look at how the results depend on chain length near the transition. Two important observations are the following:

- The peak in the specific heat gets stronger with increasing chain length. The

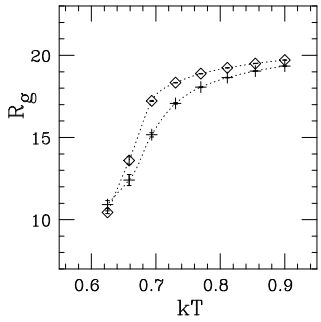

Figure 4: Radius of gyration (in Å) against temperature for the the three-helix sequence, for $\kappa = 0$ ($\diamond$) and $\kappa = 0.3$ (+).

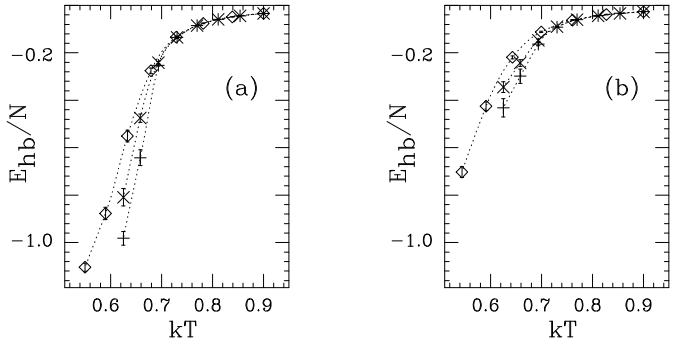

Figure 5: Hydrogen-bond energy per amino acid, $E_{\rm hb}/N$, against temperature for the sequences 1H ($\diamond$), 2H ($\times$) and 3H (+) (see Table 1), for (a) $\kappa = 0$ and (b) $\kappa = 0.3$.

increase in height is not inconsistent with a linear size dependence, which is what one would expect at a conventional first-order phase transition with a latent heat.

- The decrease in hydrogen-bond energy per amino acid, $E_{\rm hb}/N$, with decreasing temperature gets more rapid with increasing chain length, as shown in Figure 5a. This implies that the three-helix protein makes more stable secondary structure than the one- and two-helix segments.

It turns out that the sequence 3H does form a three-helix bundle at low temperatures. This bundle can have two distinct topologies; if we let the first two helices form a U, then the third helix can be either in front of or behind that U. The model is, not unexpectedly, unable to discriminate between these two possibilities. To characterize low-temperature conformations, we therefore determined two representative

Figure 6: Representative low-temperature structures, FU and BU, respectively. Drawn with RasMol [29].

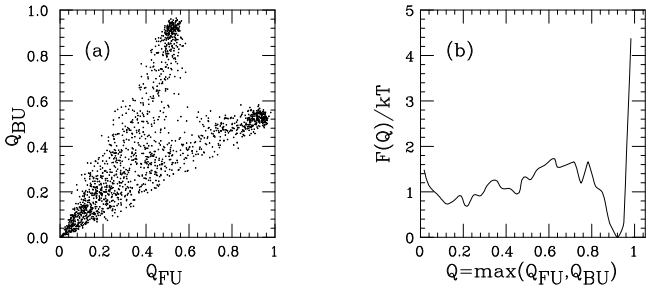

Figure 7: (a) $Q_{\rm FU}, Q_{\rm BU}$ scatter plot (see Equation 10) at the collapse temperature. (b) Free-energy profile $F(Q)$ at the same temperature.

structures, one for each topology, which, following [27], are referred to as FU and BU, respectively. These structures are shown in Figure 6. Given an arbitrary conformation, we then measure the root-mean-square deviations δ_i ($i = {\rm FU}, {\rm BU}$) from these two structures (calculated over all backbone atoms). These deviations are converted into similarity parameters Q_i by using

$$Q_i = \exp(-\delta_i^2/100\text{Å}^2)\,. \tag{10}$$

At high temperatures, both Q_i tend to be small. At low temperatures, the system spends most of its time close to one or the other of the structures FU and BU; either $Q_{\rm FU}$ or $Q_{\rm BU}$ is close to 1. Finally, at the collapse temperature, all three of these regions are populated, as can be seen from Figure 7a. In particular, this implies that folding and collapse occur at the same temperature.

In Figure 7b, we show the free-energy profile $F(Q)$ at the folding temperature, where $Q = \max(Q_{\rm FU}, Q_{\rm BU})$ is taken as a measure of "nativeness". The free energy has a relatively sharp minimum at $Q \approx 0.9$, corresponding to $\delta = \min(\delta_{\rm FU}, \delta_{\rm BU}) \approx 3$Å. This is followed by a weak barrier around $Q = 0.7$, corresponding to $\delta \approx 6$Å. Finally,

there is a broad minimum at small Q, where $Q = 0.2$ corresponds to $\delta \approx 13$Å. In [11], it was shown that the low-Q minimum corresponds to expanded structures with a varying secondary-structure content.

In particular, these results show that the three-helix sequence exhibits a first-order-like collapse transition that coincides with its folding transition. This is the behavior for $\kappa = 0$ (see Equation 9). Next we discuss the character of the collapse transition for $\kappa \neq 0$, starting with positive κ.

3.2 Dominant Hydrophobicity Forces

A positive κ means strong hydrophobicity forces and weak hydrogen bonds. For small positive κ, the collapse temperature remains approximately the same as for $\kappa = 0$. However, the transition gets weaker with increasing κ. This is illustrated in Figures 3b and 4, using data obtained for $\kappa = 0.3$.

In Figure 3b, we show the specific heat for $\kappa = 0.3$. Compared to the $\kappa = 0$ results (see Figure 3a), we see that the peak in the specific heat is lower, and that the chain-length dependence is weaker. There is no sign that the chain collapse is first-order-like for $\kappa = 0.3$.

Consistent with the data for the specific heat, we see from Figure 4 that the radius of gyration changes more slowly with temperature for $\kappa = 0.3$ than for $\kappa = 0$.

It is also interesting to look at the secondary-structure content. From Figure 5, it can be seen that the hydrogen-bond energy E_{hb} is considerably higher for $\kappa = 0.3$ than for $\kappa = 0$. In particular, the results show that the secondary-structure content at the collapse temperature is lower for $\kappa = 0.3$.

For $\kappa = 0.3$, we furthermore find that the three-helix sequence does not show structural stability at temperatures immediately below the collapse transition (data not shown), so the folding temperature is different from and lower than the collapse temperature in this case. Between these two temperatures, the chain exists in a compact (molten globule) state without specific structure.

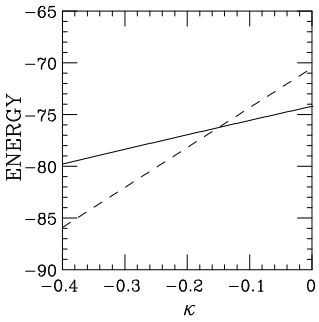

Figure 8: Three-helix-bundle (full line) and one-helix (dashed line) energies against κ (see the text).

3.3 Dominant Hydrogen Bonds

We now turn to negative κ, meaning strong hydrogen bonds and weak hydrophobicity forces. It is clear that the three-helix sequence will form one long helix rather than a helical bundle if κ is made too large negative. To get an idea of when this happens, we compare the energies of an optimized three-helix-bundle conformation and an optimized rodlike conformation, for different κ. These conformations were generated as follows.

Starting at $\kappa = 0$, we quenched a large number of low-temperature Monte Carlo conformations to zero temperature, by using a conjugate-gradient method. The structure with the lowest energy found is the BU structure in Figure 6. This structure is taken as our three-helix-bundle conformation at $\kappa = 0$. Our rodlike $\kappa = 0$ conformation was also obtained by a conjugate-gradient minimization, starting from a long "ideal" helix.

We then performed energy minimizations at successively lower κ, each time taking the optimized conformations from the previous κ as our two starting points. The two sets of energies obtained this way are shown as functions of κ in Figure 8. We see that the curves cross at $\kappa \approx -0.15$. Although there may well exist three-helix-bundle energies that are somewhat lower than those in Figure 8, these results strongly suggest that the ground state turns into one long helix already at a relatively small negative κ.

4 Summary

The calculations discussed in this paper can be divided into two parts. First, we showed that the three-helix-bundle protein, for a suitable choice $(\tilde{\epsilon}_{\rm hb}, \tilde{\epsilon}_{\rm AA})$ of the parameters $(\epsilon_{\rm hb}, \epsilon_{\rm AA})$, indeed has the properties listed in the introduction. Let us stress that we find these properties without resorting to the Gō approximation. This is important as many current models rely on this approximation [6, 17–21], based on the view that the folding properties are strongly influenced by the native topology, whereas energetic frustration plays a less important role. The results presented in this paper are consistent with this view, but it is clear that further studies are needed in order to properly understand the consequences and applicability of the Gō approximation.

In the second part, we presented results obtained for $(\epsilon_{\rm hb}, \epsilon_{\rm AA}) = (\tilde{\epsilon}_{\rm hb} - \kappa, \tilde{\epsilon}_{\rm AA} + \kappa)$ for different κ. Not unexpectedly, it turns out that the folding behavior depends critically on the relative strength of the parameters $\epsilon_{\rm hb}$ and $\epsilon_{\rm AA}$. In particular, we saw that a first-order-like collapse to a three-helix-bundle state is observed only in a narrow window around $\kappa = 0$; a proper balance between hydrogen bonds and hydrophobicity forces is required for the chain to show this behavior.

The fact that the dependence on these parameters is strong may seem unwanted, but is not physically unreasonable. In fact, the situation is somewhat reminiscent of what has been found for homopolymers with stiffness [30–33], with the hydrogen bonds playing the role of the stiffness term. Note also that the incorporation of full side chains will make the chains intrinsically stiffer, which might lead to a weaker dependence on the hydrogen-bond strength $\epsilon_{\rm hb}$.

Acknowledgements

This work was in part supported by the Swedish Foundation for Strategic Research.

References

[1] Gō, N. and Taketomi H.: Respective roles of short- and long-range interactions in protein folding, *Proc. Natl. Acad. Sci. USA* **75** (1978), 559–563.

[2] Săli, A., Shakhnovich, E. and Karplus, M.: Kinetics of protein folding: A lattice model study of the requirements for folding to the native state, *J. Mol. Biol.* **235** (1994), 1614–1636.

[3] Bryngelson, J.D., Onuchic, J.N., Socci, N.D. and Wolynes, P.G.: Funnels, pathways, and the energy landscape of protein folding: A synthesis, *Proteins: Struct. Funct. Genet.* **21** (1995), 167–195.

[4] Dill, K.A. and Chan, H.S.: From Levinthal to pathways to funnels, *Nature Struct. Biol.* **4** (1997), 10–19.

[5] Klimov, D.K. and Thirumalai, D.: Linking rates of folding in lattice models of proteins with underlying thermodynamic characteristics, *J. Chem. Phys.* **109** (1998), 4119–4125.

[6] Nymeyer, H., García, A.E. and Onuchic, J.N.: Folding funnels and frustration in off-lattice minimalist protein landscapes, *Proc. Natl. Acad. Sci. USA* **95** (1998), 5921–5928.

[7] Socci, N.D., Bialek, W.S. and Onuchic, J.N.: Properties and origins of protein secondary structure, *Phys. Rev. E* **49** (1994), 3440–3443.

[8] Irbäck, A., Peterson, C., Potthast, F. and Sommelius, O.: Local interactions and protein folding: A three-dimensional off-lattice approach, *J. Chem. Phys.* **107** (1997), 273–282.

[9] Vendruscolo, M., Najmanovich, R. and Domany, E.: Protein folding in contact map space, *Phys. Rev. Lett.* **82** (1999), 656–659.

[10] Alm, E. and Baker, D.: Matching theory and experiment in protein folding, *Curr. Opin. Struct. Biol.* **9** (1999), 189–196.

[11] Irbäck, A., Sjunnesson, F. and Wallin, S.: Three-helix-bundle protein in a Ramachandran model, *Proc. Natl. Acad. Sci. USA* **97** (2000), 13614–13618.

[12] Ramachandran, G.N. and Sasisekharan, V.: Conformation of polypeptides and proteins, *Adv. Protein Chem.* **23** (1968), 283–437.

[13] Regan, L. and DeGrado, W.F.: Characterization of a helical protein designed from first principles, *Science* **241** (1988), 976–978.

[14] Lyubartsev, A.P., Martsinovski, A.A., Shevkunov, S.V. and Vorontsov-Velyaminov, P.V.: New approach to Monte Carlo calculation of the free energy: Method of expanded ensembles, *J. Chem. Phys.* **96** (1992), 1776–1783.

[15] Marinari, E. and Parisi, G.: Simulated tempering: A new Monte Carlo scheme, *Europhys. Lett.* **19** (1992), 451–458.

[16] Irbäck, A. and Potthast, F.: Studies of an off-lattice model for protein folding: Sequence dependence and improved sampling at finite temperature, *J. Chem. Phys.* **103** (1995), 10298–10305.

[17] Shea, J.-E., Nochomovitz, Y.D., Guo, Z. and Brooks, C.L., III: Exploring the space of protein folding Hamiltonians: The balance of forces in a minimalist β-barrel model, *J. Chem. Phys.* **109** (1998), 2895–2903.

[18] Shea, J.-E., Onuchic, J.N. and Brooks, C.L., III: Exploring the origins of topological frustration: Design of a minimally frustrated model of fragment B of protein A, *Proc. Natl. Acad. Sci. USA* **96** (1999), 12512–12517.

[19] Clementi, C., Jennings, P.A. and Onuchic, J.N.: How native-state topology affects the folding of dihydrofolate reductase and interleukin-1/β, *Proc. Natl. Acad. Sci. USA* **97** (2000), 5871–5876.

[20] Clementi, C., Nymeyer, H. and Onuchic, J.N.: Topological and energetic factors: What determines the structural details of the transition state ensemble and "en-route" intermediates for protein folding? An investigation for small globular proteins, *J. Mol. Biol.* **298** (2000), 937–953.

[21] Shimada, J., Kussell, E.L. and Shakhnovich, E.I.: The folding thermodynamics and kinetics of crambin using an all-atom Monte Carlo simulation, *J. Mol. Biol.* **308** (2001), 79–95.

[22] Rey, A. and Skolnick, J.: Computer modeling and folding of four-helix bundles, *Proteins: Struct. Funct. Genet.* **16** (1993), 8–28.

[23] Guo, Z. and Thirumalai, D.: Kinetics and thermodynamics of folding of a *de novo* designed four-helix bundle protein, *J. Mol. Biol.* **263** (1996), 323–343.

[24] Zhou, Z. and Karplus, M.: Folding thermodynamics of a model three-helix-bundle protein, *Proc. Natl. Acad. Sci. USA* **94** (1997), 14429–14432.

[25] Koretke, K.K., Luthey-Schulten, Z. and Wolynes, P.G.: Self-consistently optimized energy functions for protein structure prediction by molecular dynamics, *Proc. Natl. Acad. Sci. USA* **95** (1998), 2932–2937.

[26] Hardin, C., Luthey-Schulten, Z. and Wolynes, P.G.: Backbone dynamics, fast folding, and secondary structure formation in helical proteins and peptides, *Proteins: Struct. Funct. Genet.* **34** (1999), 281–294.

[27] Takada, S., Luthey-Schulten, Z. and Wolynes, P.G.: Folding dynamics with non-additive forces: A simulation study of a designed helical protein and a random heteropolymer, *J. Chem. Phys.* **110** (1999), 11616–11629.

[28] Ferrenberg, A.M. and Swendsen, R.H.: New Monte Carlo for studying phase transitions *Phys. Rev. Lett.* **61** (1988), 2635–2638; *Phys. Rev. Lett.* **63**, 1658 (Erratum), and references given in the erratum.

[29] Sayle, R. and Milner-White, E.J.: RasMol: Biomolecular graphics for all, *Trends Biochem. Sci.* **20** (1995), 374–376.

[30] Kolinski, A., Skolnick, J. and Yaris, R.: Monte Carlo simulations on an equilibrium globular protein folding model, *Proc. Natl. Acad. Sci. USA* **83** (1986), 7267–7271.

[31] Doniach, S., Garel, T. and Orland, H.: Phase diagram of a semiflexible polymer chain in a θ solvent: Application to protein folding, *J. Chem. Phys.* **105** (1996), 1601–1608.

[32] Bastolla, U. and Grassberger, P.: Phase transitions of single semi-stiff polymer chains, *J. Stat. Phys.* **89** (1997), 1061–1078.

[33] Doye, J.P.K., Sear, R.P. and Frenkel, D.: The effect of chain stiffness on the phase behaviour of isolated homopolymers, *J. Chem. Phys.* **108** (1998), 2134–2142.